JOURNAL OF GEOPHYSICAL RESEARCH, VOL. 102, NO. A4, PAGES 7477–7484, APRIL 1, 1997

VLF remote sensing of high-energy auroral particle precipitation

S. A. Cummer, T. F. Bell, and U. S. Inan

Space, Telecommunications and Radioscience Laboratory, Stanford University, Stanford, California

D. L. Chenette

Lockheed Martin Palo Alto Research Laboratory, Palo Alto, California

Abstract. Ground-based measurements of VLF transmitter signals propagating in the Earth-ionosphere waveguide can be used to determine the location of nighttime high-energy ($\gtrsim$100 keV) auroral particle precipitation. When the region of auroral particle precipitation passes over a VLF propagation path, disturbances in the D region of the ionosphere created by the high-energy particles perturb the amplitude of VLF signals propagating below in a characteristic manner. Continuous nighttime observations of the amplitude of the signal from the NLK transmitter (24.8 kHz, Jim Creek, Washington) were made in Gander, Newfoundland, during November 1993 and January 1994. Simultaneous images of atmospheric X rays created by auroral particle precipitation taken by the AXIS instrument on the UARS satellite were examined for times when large-scale auroral particle precipitation extended over the NLK-Gander propagation path. Quantitative characteristics of the precipitation-associated NLK signal perturbations are established from days which clearly exhibit good correlation between the AXIS images and VLF data, and a larger data set from the months of November 1993 and January 1994 is examined statistically to determine the effectiveness of the VLF technique in capturing particle precipitation events. The number of particle precipitation onsets seen in the AXIS images that can be readily identified in the VLF amplitude data is found to be almost 94%. VLF propagation model calculations show that the observed VLF amplitude decreases are consistent with propagation under conditions of enhanced lower ionosphere electron density caused by auroral electron precipitation and suggest that electrons with energies greater than 100 keV are responsible for the VLF amplitude perturbations.

Introduction

We investigate the utility of a new technique to detect the edge of the auroral particle precipitation region using ground-based observations of signals from VLF transmitters. This method directly detects D region ionospheric disturbances caused by high-energy (>100 keV) auroral particle precipitation, and provides information on both the large-scale extent of the precipitation region and the intensity of the associated electron density perturbations in the lower ionosphere.

Observations of both of these quantities are important for practical and scientific reasons. Communication (from VLF to HF) and navigation systems (e.g., Loran-C and Omega) can be significantly affected by these ionospheric perturbations [*Swanson*, 1983; *Inan et al.*, 1985]. Such high-energy precipitation can also cause significant changes in the chemistry of the lower ionosphere [*Callis et al.*, 1991; *Baker et al.*, 1993]. Beyond the direct ionospheric effects of the precipitation, previous work has indicated that the equatorward boundary of high-energy auroral particle precipitation is often coincident with the low-latitude boundary of the auroral electrojet current system [*Cummer et al.*, 1996; *Kikuchi and Evans*, 1983], which can cause severe problems with electric power delivery systems during magnetic disturbances [*Ringlee*, 1989].

The relationship between subionospheric VLF phase perturbations and large scale energetic particle precipitation has been previously investigated. *Potemra and Rosenberg* [1973] found that nighttime VLF phase advances on multiple midlatitude paths occurred simultaneously with the onset of a magnetospheric substorm. *Kikuchi and Evans* [1983], using a combination of ground-based VLF phase measurements, ground magnetometer observations, and satellite particle precipitation data, found that the occurrence of VLF phase anomalies on high-latitude signals is well-correlated with an increase in the precipitation of > 300 keV electrons at the same latitudes. However, neither of these studies had available a measure of precipitation directly

Paper number 96JA03721.
0148-0227/97/96JA-03721$09.00

over the VLF propagation path and thus were not able to draw any definitive conclusions about the effects of precipitation on the VLF signal.

To examine these effects in detail, we compare VLF amplitude data with X ray images of the northern auroral precipitation region from the atmospheric X ray imaging spectrometer (AXIS) on the UARS satellite [*Winningham et al.*, 1993], with the aim of determining whether recognizable amplitude perturbations in the VLF signal occur when particle precipitation appears over the VLF propagation path. We are primarily concerned with detecting the location of the precipitation region rather than investigating the energetics of the precipitation, but precipitating energy spectra are discussed briefly in the numerical modeling section below. Our data set consists of observations from 50 nights (covering most of November 1993 and January 1994) with complete VLF amplitude records and a complete set of AXIS images over the proper geographic region. A data set of this size is large enough to determine whether the VLF technique described herein can reliably monitor the position of the high-energy auroral particle precipitation region. Our use of the term auroral particle precipitation refers to the relatively steady precipitation associated with the diffuse aurora.

Description of the VLF Data

Throughout the study period, we continuously measured the amplitude of the subionospheric signal from the NLK transmitter (24.8 kHz) in Jim Creek, Washington, with a narrow-band (500 Hz bandwidth) receiver in Gander, Newfoundland. Figure 1 shows an overhead geographic view of the great circle propagation path as well as the lines of constant geomagnetic latitude corresponding to $L = 7$ ($\sim 68°$) and $L = 4$ ($\sim 60°$). The positions of these lines show that the NLK-GA propagation path is situated such that during geomagnetically quiet times, any auroral particle precipitation would likely lie north of the propagation path, while during disturbed times the precipitation would fall directly on or even south of the path.

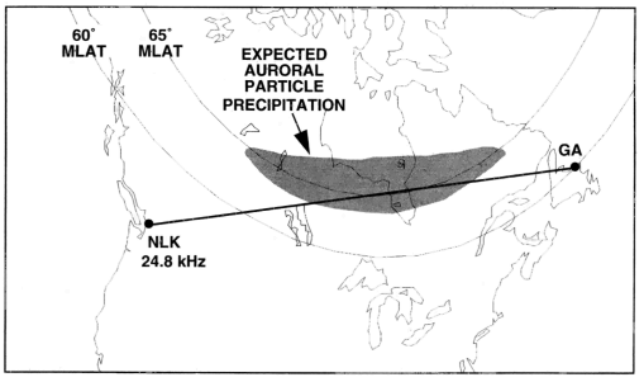

Figure 1. An overhead geographic view of the VLF propagation path from NLK to Gander, Newfoundland used in this study. The signal is generated by a transmitter in Washington state (NLK) and is measured by a receiver in Gander. Two representative lower-latitude boundaries for the auroral oval are shown, one at 65° geomagnetic latitude corresponding to quiet times and one at 60° corresponding to a moderate magnetic storm. The path is situated such that during quiet times the great circle propagation path would not be crossed by the auroral oval, but any auroral expansion would likely extend it over the path, affecting the NLK signal.

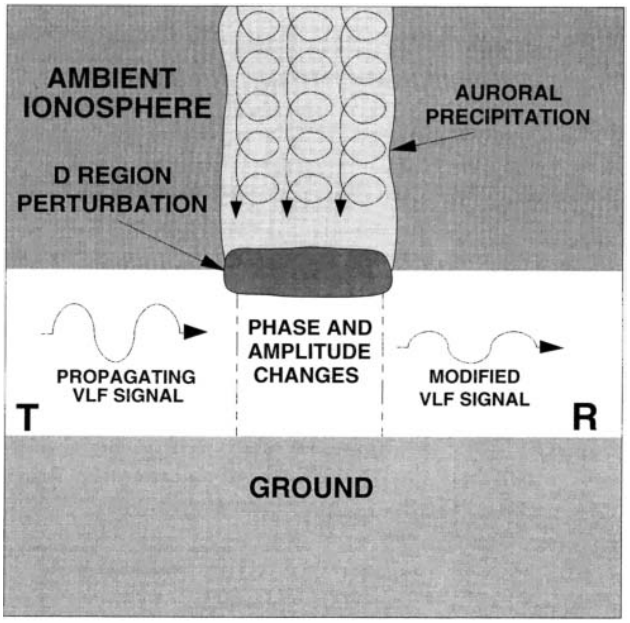

Figure 2. The mechanism of the particle precipitation-VLF interaction is schematically shown above. A ground VLF transmitter (T) launches a CW signal into the Earth-ionosphere waveguide. The waveguide signal propagating under the region of the auroral incursion is modified due to the conductivity changes in the ionosphere caused by the high-energy electron precipitation. The penetration of the precipitation over the propagation path is observed at the receiver (R) as phase and amplitude variations in the VLF signal.

Subionospheric VLF propagation is well known to be very sensitive to D region ionospheric parameters [*Galejs*, 1972]. This sensitivity is due to the fact that the bulk of VLF wave energy is reflected at ~80-90 km altitudes, in the nighttime D region. Changes in the D region electron density caused by high-energy auroral particle precipitation are manifested as perturbations in the VLF signal propagating under the disturbed ionosphere. High-energy precipitation (>50 keV, although it depends somewhat on the ambient density of the atmosphere) is necessary for these ionospheric disturbances to extend below 90 km, as lower-energy electrons do not penetrate to these altitudes [*Rees*, 1989]. Figure 2 shows a schematic description of this process.

VLF propagation is much less sensitive to D region disturbances during the day because the daytime D region electron density is much higher than that at night, which both lowers the VLF reflection height below the main part of these disturbances and reduces the relative magnitude of the electron density perturbations caused by precipitating energetic particles. For this reason, we only investigate nighttime auroral particle precipitation in this paper.

"Quiet Night" Behavior of the NLK-GA Signal

In order to identify the NLK amplitude perturbations caused by auroral expansion, we calculate an average "quiet" night curve to show the expected NLK nighttime amplitude variation in he absence of any auroral effects. Of the 50 nights included in our study, 16 of them (eight in November and eight in January) had $K_P < 3$ for each 3-hour period between 0000 and 1200 UT, indicating low enough geomagnetic activity so that any auroral particle precipitation was likely located north of the VLF propagation path. The data from these nights were averaged after time shifting to align them relative to sunset at the NLK transmitter. The time shift is necessary to ensure that any nonauroral local time effects caused by the disappearance of ionizing solar radiation over the path are included as part of the quiet night pattern. Figure 3 shows the NLK amplitude quiet night variation along with the standard deviation to demonstrate the typical deviation from the quiet night curve.

The quiet night curve established as described above is subtracted from the VLF data from the other nights (after appropriate time alignment relative to sunset on each day) to show the variation from the quiet night values caused by the auroral expansion over the propagation path. The quiet night selection criterion based on K_P is not ideal, as some of these "quiet" nights showed some apparent auroral activity. However, these were in the minority, and their effect on the quiet night curve is very minimal.

Description of AXIS Images

To independently determine the days on which the auroral precipitation region expanded over the NLK-Gander propagation path, we examine images of the auroral region from the atmospheric X ray imaging spectrometer (AXIS) on the UARS satellite [*Winningham et al.*, 1993]. AXIS measures X rays emanating from the atmosphere across a narrow strip extending from limb to limb perpendicular to the UARS ground track. An image is accumulated "push-broom" style as the spacecraft orbits the Earth. The measured X rays are in the energy range from 3 keV to 100 keV. However, the sensitivity of the detector, the intensity of the precipitating electron flux, and the resulting intensity of the X ray source spectrum decrease rapidly with increasing energy above a few tens of keV. As a result, AXIS is most sensitive to electrons with energies from ~5 keV to ~20 keV.

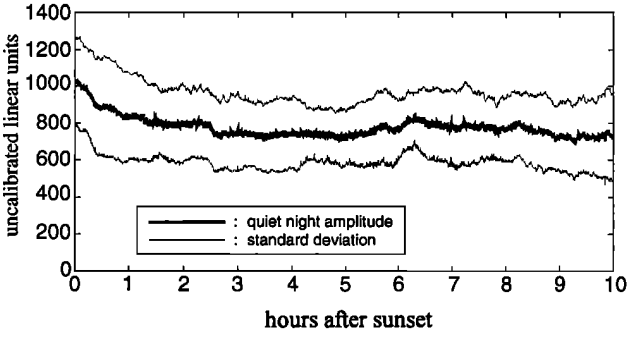

Figure 3. The quiet night variation of the NLK (24.8 kHz) amplitude received at Gander. The amplitude is in uncalibrated linear sampling units. The lighter lines indicate the standard deviation of the amplitude over the 16 quiet nights.

For this study, we used images of the total X ray count (background levels have been subtracted) during UARS passes over the NLK-GA propagation path. These images show the position of the auroral electron precipitation, and from these we can determine if there is significant electron precipitation over the VLF propagation path. AXIS images have been used previously to calculate atmospheric energy input and ionization during a geomagnetic storm [*Chenette et al.*, 1993].

Simultaneous VLF Amplitude Data and AXIS Images

We now show data from three different days on which well-defined NLK amplitude perturbations were observed at Gander at the same time as AXIS X ray images show significant particle precipitation over the NLK-GA path. The VLF amplitude data are shown as percentage deviation from the quiet night curve. The shaded sections of the VLF amplitude curves correspond to the times of the AXIS images shown above the VLF data, and the VLF amplitude events (identified as described below) are marked by arrows.

Plate 1 shows the data from January 16, 1994. The NLK-GA amplitude deviated very little from the quiet night curve until 0810 UT, when the amplitude began to sharply drop, reaching a minimum at 0830 UT and remaining significantly depressed for more than 1 hour. The AXIS images show precipitation north of the NLK-GA path between 0500 and 0530 UT, almost no precipitation between 0630 and 0700 UT, and a significant region of precipitation directly over the path between 0815 and 0845 UT (when the NLK-GA amplitude had reached a minimum).

Plate 2 shows the data from November 10, 1993. The combined data on this night was qualitatively very similar to that from January 16, 1994. The NLK-GA amplitude deviation from the quiet night was quite small until 0600 UT, when the amplitude began to drop significantly over the course of an hour. The amplitude remained low through the remainder of the night. The AXIS images show no precipitation from 0445 to 0515 UT, but a region of precipitation had appeared by 0615-0645 UT when the VLF amplitude was dropping. The image from 0750 to 0820 UT still shows significant precipitation over the path, while the VLF amplitude remained at an unusually low level.

Plate 3 shows the data from January 19, 1994. The VLF data show an amplitude drop early in the night at 0225 UT (well before local midnight at the center of the path), a recovery to quiet night levels, and another VLF event at 0550 UT. The hypothesis that these

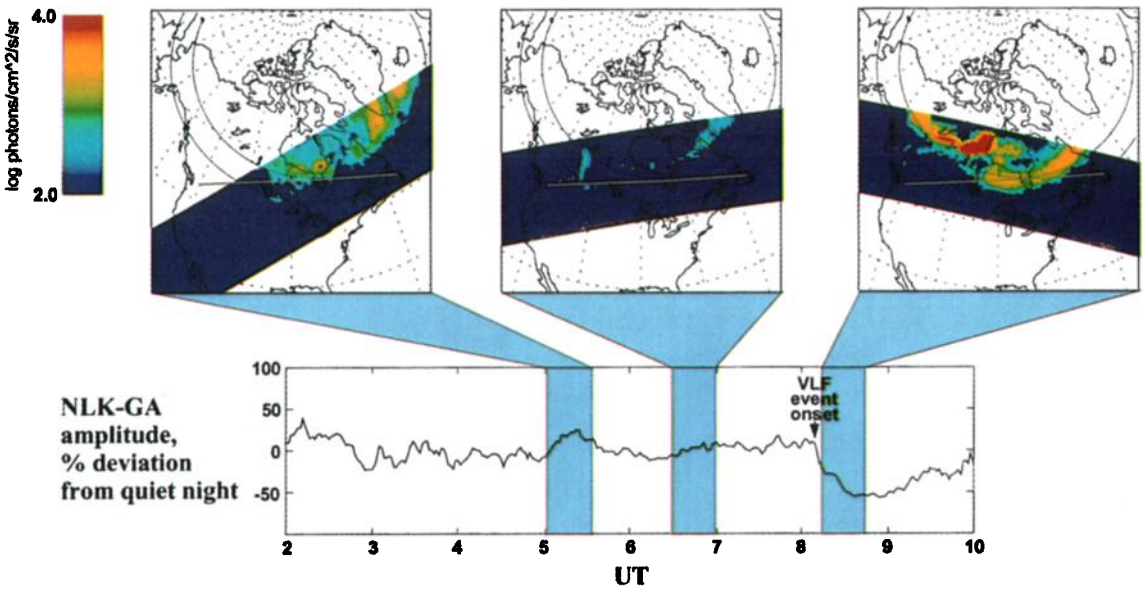

Plate 1. Simultaneous NLK-GA amplitude data and AXIS images for January 16, 1994. The NLK-GA propagation path is marked by a gray line in the images. There is a strong drop in the NLK-GA amplitude data beginning at 0810 UT, and the simultaneous AXIS image shows a significant particle precipitation region had appeared directly over the path.

drops are caused by particle precipitation over the path is supported by the AXIS images, which show a small amount of precipitation over the path from 0330 to 0400 UT, none from 0510 to 0540 UT, and the reappearance of the precipitation from 0645 to 0715 UT.

Evaluated on their own, these three nights of data strongly suggest that significant drops in the amplitude of the NLK-GA signal are associated with energetic particle precipitation directly over the VLF great-circle propagation path as seen in the AXIS images. In the next section, we evaluate a larger data set from 50 nights to more thoroughly demonstrate this association.

Statistics

All of the VLF perturbations associated with the onset of precipitation over the path shown in Plates 1-3 exhibit certain repeatable characteristics, most notably the significant amplitude decrease. Using data from days with clear VLF/AXIS correlations (such as those shown above), we determined a set of quantitative criteria for the identification of a VLF amplitude perturbation associated with auroral particle precipitation. In units of percent deviation from the quiet night curve, a "VLF event" is defined as an absolute amplitude drop from above -5% to below -35% with an average slope steeper than -35% per hour. A VLF event onset is defined as the start of the amplitude drop defining a VLF event. As these criteria are meant to be broad enough to encompass all of the precipitation-associated VLF amplitude events, we did not use superposed epoch analysis to determine the average event parameters but rather took the broadest parameters from the days with a good VLF/AXIS match and perturbed them slightly to provide a good match between all of the VLF and AXIS data.

We examined all of the available VLF data during the study period (November 1993 and January 1994) and identified all VLF events that met the above described criteria. We also examined the complete set of AXIS images when the satellite passed over the NLK-GA path for cases in which X ray fluxes greater than 10^3 photons cm^{-2} s^{-1} sr^{-1} (implying significant particle precipitation) were observed directly over the VLF propagation path. On most of the days in this study, AXIS images of the region of interest were obtained approximately every 1.6 hours between 0200 and 1000 UT. These two sets of events were then compared to determine the effectiveness of the VLF amplitude data in identifying the onset of large-scale auroral particle precipitation over the path.

In the 50 nights studied, there were a total of 39 VLF amplitude events which occurred during periods when UARS was in a position to make X ray images over the path. Some of these nights showed more than one VLF event. During the same 50 days, there were 42 AXIS images which showed significant particle precipitation over the path. When two consecutive AXIS images showed the onset of precipitation (defined as no significant X ray flux in the first but X ray flux greater than 10^3 photons cm^{-2} s^{-1} sr^{-1} over the path in the second), we noted whether a VLF event that was more than halfway between the event onset and the threshold (-35%) crossing had occurred between the times of these two images. Additionally, after the "halfway" point of all VLF events, we noted whether the subsequent AXIS image showed significant precipitation over the VLF path. This latter method of comparison was found to be useful because UARS sometimes passed over the region of interest just after the onset of a VLF event, and the low-energy X ray emission was still weak and did not show up above the background in the AXIS

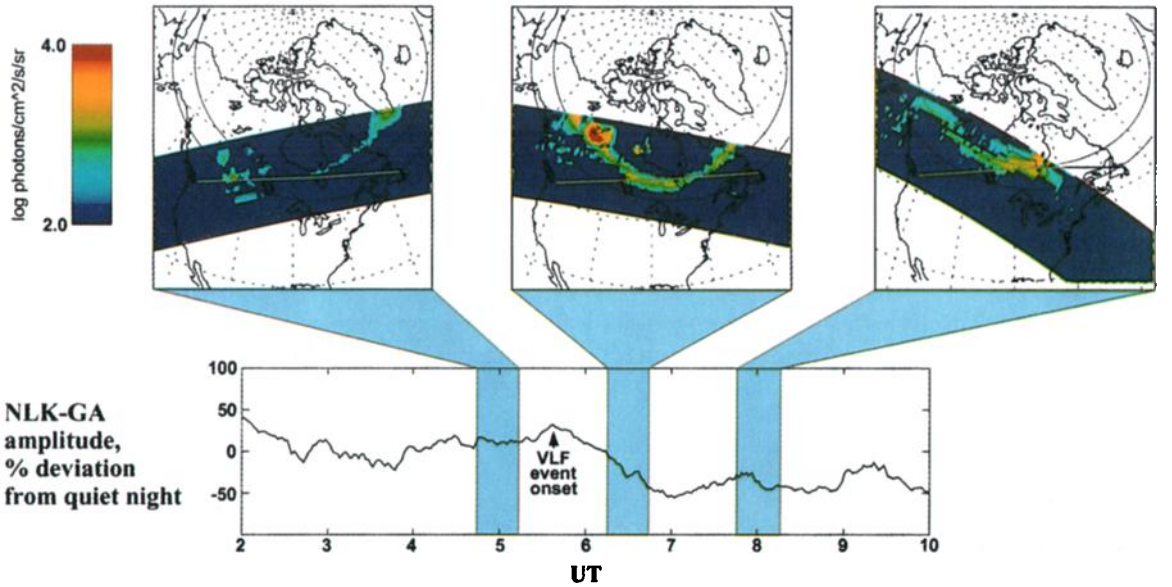

Plate 2. Simultaneous NLK-GA amplitude data and AXIS images for November 10, 1993. The NLK-GA propagation path is marked by a gray line in the images. A steady drop in the NLK-GA amplitude data began at 0600 UT, while the AXIS image from 0615 to 0645 UT shows that significant particle precipitation had developed directly over the path. Both the amplitude drop and precipitation over the path persisted for more than 3 hours.

images, suggesting that the precipitation at these early times was dominated by >100 keV electrons. By comparing the images to the times when VLF events are halfway through their amplitude drops, we increase the likelihood that the precipitation over the path is strong enough to show up in the AXIS images.

The VLF and AXIS data sets were compared in these two ways. For the first comparison, there were a total of 16 pairs of AXIS images which showed the required precipitation onset signature. In 15 of the 16 pairs, a VLF event was more than halfway between onset and threshold at some time between the two image times, indicating that almost 94% of the precipitation event onsets seen in the AXIS images are also seen in the VLF amplitude data.

The second comparison shows that of the 39 VLF events for which UARS was in a good position, the subsequent AXIS images showed precipitation directly over

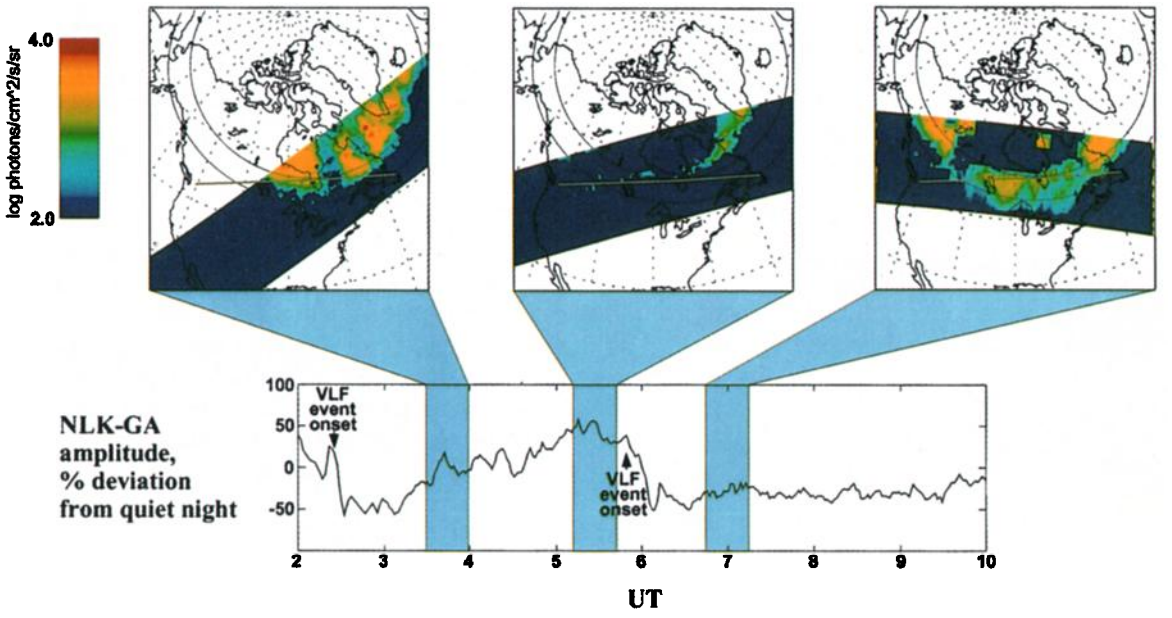

Plate 3. Simultaneous NLK-GA amplitude data and AXIS images for January 19, 1994. The NLK-GA propagation path is marked by a gray line in the images. This night shows two distinct VLF amplitude drops, and the AXIS images show the disappearance and reappearance of significant particle precipitation over the path consistent with the times of the VLF amplitude drops.

the path 27 times (69%). For the 12 cases in which the post-VLF-event AXIS image did not show significant precipitation over the path, three of the subsequent AXIS images did show significant precipitation just north of the VLF propagation path, indicating that there may well have been high energy precipitation over the path that did not show up in the AXIS images. Also, in two of these cases, by the time the subsequent AXIS image was made, the VLF amplitude had recovered from the drop and was within 10% of the quiet night curve, indicating the possible disappearance of the precipitation. Excluding these uncertain events from the comparison would boost the agreement percentage to 79%. The reason for the lack of correlation of the remaining seven VLF events with precipitation in the AXIS images is not clear. Given that observations sometimes indicated a delay between the onset of >100 keV precipitation (as seen in the VLF data) and the ~10 keV precipitation (from the AXIS images), it seems plausible that >100 keV precipitation could be present without significant ~10 keV precipitation that would show up in the AXIS images.

The results from both of these two comparisons are summarized in Table 1. The good agreement between AXIS event onset image pairs and VLF events indicate that the VLF method does capture essentially every precipitation event over the path. VLF phase data were unavailable for the NLK-GA path during this time period, but simultaneous phase measurements would provide an additional criterion for the identification of VLF events [*Cummer et al.*, 1996] and could significantly reduce the identification of VLF events not associated with auroral particle precipitation.

The fact that nearly every AXIS event onset image pair corresponds to a VLF event also suggests that the locations of the high-energy precipitation (that responsible for the VLF events because of the penetration depth required to cause D region disturbances [*Rees*, 1989]) and ~ 10 keV precipitation (that responsible for the majority of the X rays seen by AXIS) are often coincident. A further examination of particle data from UARS should provide more definite evidence for this assertion.

VLF Propagation Modeling

We now theoretically model VLF propagation from NLK to GA in an effort to determine whether the observed precipitation-associated VLF amplitude signatures are consistent with the ionospheric changes under auroral electron precipitation. The model employed is the LWPC VLF propagation code [*Ferguson and Snyder*, 1987], which we apply to the January 16, 1994, 0820-0830 UT time period (shown above in Plate 1). The AXIS image clearly shows that the diffuse auroral emission region lay directly over the NLK-GA propagation path at this time, and we estimate that the precipitation covered a 1500-km-long segment of the path. The instrument imaged this X ray emission region from 0827 to 0835 UT, during which period the VLF amplitude was relatively constant at its perturbed value, so we assume that the precipitation did not significantly change location or intensity during this period.

Table 1. Statistical Comparison of AXIS Images and VLF Events

Event	Number
AXIS image pair showing precipitation onset	16
AXIS image pair showing precipitation onset with VLF event between image times	15 (94%)
VLF event	39
VLF event with subsequent AXIS image showing significant precipitation	27 (69%)

We assume an undisturbed D region electron density profile from *Reagan et al.* [1981], which has provided good results in conjunction with the LWPC VLF propagation model in previous work [*Lev-Tov et al.*, 1995] and is representative of an undisturbed midlatitude to high-latitude profile. The electron-neutral collision frequency used was taken from *Thomson* [1993], and it is assumed to be unaffected by the auroral electron precipitation. We use two different estimates of the energy spectrum for the precipitating electrons: one is a precipitating electron spectrum spectrum with a $1/E$ falloff in energy extrapolated from NOAA 6 spacecraft data reported by *Kikuchi and Evans* [1983], and the other comes from an inversion of the AXIS X ray energy measurements to extract electron energy flux as detailed by *Chenette et al.* [1993] and is thus an indirect measurement of the actual precipitating flux during the time of interest. However, the source of the atmospheric X rays detected by AXIS is primarily electrons in the 10 keV energy range, so assuming an exponential energy spectrum (as is done) probably underestimates the precipitation above 100 keV. We calculate VLF amplitude perturbations using both profiles to highlight the differences expected from different precipitating spectra.

The two precipitating energy spectra are plotted in Figure 4a, and Figure 4b shows the ambient D region electron density profile and the two perturbed profiles under each of the two different precipitating spectra. The center of the perturbed segment is assumed to be the point of highest geomagnetic latitude on the path. These perturbed profiles were calculated using the ion-pair production model of *Rees* [1963] combined with the D region chemistry model of *Glukhov et al.* [1992].

Figure 5 shows the calculated NLK signal amplitude at Gander as a function of the length of the segment of perturbed ionosphere over the path for both disturbed profiles. As the NOAA 6 perturbed profile spreads over the path, the NLK-GA amplitude climbs very slightly until the segment length reaches 1000 km, after which the amplitude drops strongly. At an incursion length of 1500 km, the predicted signal level is down to approximately 60% of the unperturbed signal level. In contrast, as the AXIS-extracted perturbed profile spreads over the path, the NLK-GA amplitude steadily increases and reaches a peak almost 50% greater than the unperturbed signal level. With the NOAA 6 precipitat-

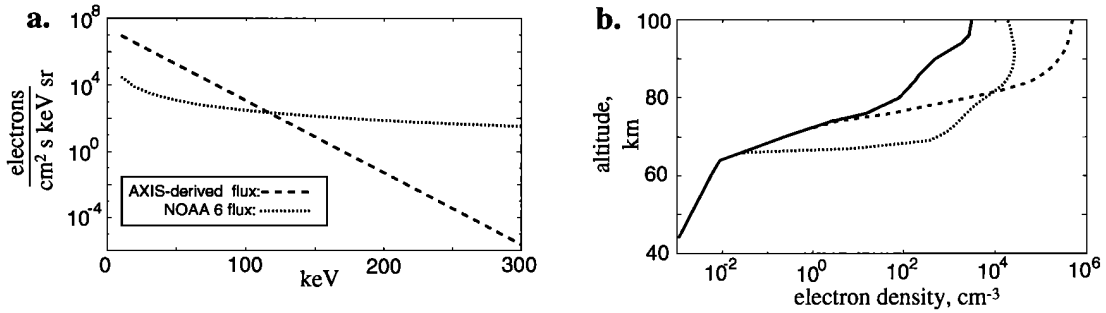

Figure 4. (a) The two precipitating energy spectra described in the text. (b) The ambient electron density profile and the calculated perturbed profiles under each precipitating spectrum in Figure 4a. The greater high-energy precipitation in the NOAA 6 spectrum leads to electron density enhancement at lower altitudes.

ing spectrum, both the shape and magnitude of this predicted signature are in good agreement with the observed data (see Plate 1), and we conclude that on January 16, 1994, the actual precipitating spectrum and associated perturbed electron density profile were similar to those observed by NOAA 6 and shown in Figure 4.

These simulations also suggest that it is those electrons with energies greater than 100 keV that are responsible for the observed VLF amplitude perturbations. Figures 4 and 5 show that the >100 keV electrons create electron density enhancement below 75 km, and this low-altitude enhancement leads to the good agreement between the propagation model results and the observations presented above.

Summary and Conclusions

We have examined the possibility of determining the location and time of occurrence of high-energy auroral particle precipitation using ground-based measurements of VLF transmitter signals. High-energy precipitation causes electron density enhancements in the D region of the ionosphere at the edge of the auroral oval, which in turn affect VLF waves propagating in the Earth-ionosphere waveguide.

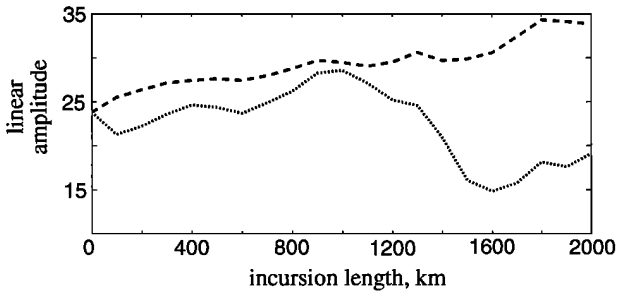

Figure 5. Plots of the modeled NLK-GA amplitude as a function of incursion length of the perturbed ionospheric profiles shown in Figure 4b. The AXIS-derived profile is in poor qualitative agreement with the observed amplitude drops. However, the NOAA 6 profile produces an amplitude drop of 40% when the perturbed segment length is 1500 km, which is in very good agreement with the observed amplitude drop (50% with an incursion of ~1500 km) on January 16, 1994.

We compared the VLF amplitude data to AXIS X ray images of the auroral oval and found excellent agreement between the two data sets: when consecutive AXIS images showed the onset of precipitation over the path, VLF amplitude events (as defined by quantitative criteria described above) were seen between the two AXIS image times in 94% of the cases studied. Of the 39 VLF events in the 50-day study period, 69% were found to be associated with particle precipitation over the path as seen in the subsequent AXIS image. This statistical comparison shows that the VLF technique captures nearly every auroral particle precipitation event seen in the AXIS images, and with good confidence an observed VLF event implies the presence of particle precipitation over the VLF propagation path.

VLF propagation from NLK to Gander was theoretically modeled using two enhanced electron density profiles calculated from two different precipitating electron energy spectra. The model calculation which used a spectrum with a $1/E$ falloff in energy, which was extrapolated from observed data reported by *Kikuchi and Evans* [1983], gave very good agreement with the observations, thereby providing a good estimate of both the precipitating energy spectrum and the associated perturbed D region electron density profile. A comparison of the results using these two precipitating spectra suggests that electrons with energies greater than 100 keV that cause the observed VLF amplitude perturbations.

The advantages of this VLF-based method are that it can provide large-scale measurements with a single receiving station on the ground and that it provides a direct measurement of the effects of auroral particle precipitation on electron density from altitudes from about 60 to 90 km. The data presented also suggest that the high-energy particle precipitation responsible for the VLF events is almost always coincident with the medium energy (~10 keV) precipitation seen in the AXIS X ray images.

We conclude that auroral expansion across the NLK-GA path can be detected by measurement of the associated amplitude signatures on the VLF signal caused by D region conductivity changes. A system with multiple receiving stations and transmitters with VLF paths

that cross through or near the auroral oval could potentially be an effective means of imaging the location of auroral precipitation on a global scale and could provide data continuously during local night.

Acknowledgments. The VLF work was supported by the Office of Naval Research under grant N00014-92-J-1579 and the associated AASERT supplement N00014-93-1-1201. The installation and operation of the VLF receiver and acquisition system at Gander, Newfoundland, was made possible by the cooperation of the 770 Communications Research Squadron of the Canadian Forces in Gander. The AXIS analysis was supported, in part, through the Particle Environment Monitor Investigation, J. D. Winningham, P. I., under SwRI subcontract NAS5-27753/17167 to Lockheed Martin, and by the Lockheed Martin Internal Research Program. We also wish to thank Victor Pasko for his assistance with the electron precipitation simulations.

The Editor thanks V. S. Sonwalkar and J. D. Winningham for their assistance in evaluating this paper.

References

Baker, D. N., R. A. Goldberg, F. A. Herrero, J. B. Blake, and L. B. Callis, Satellite and rocket studies of relativistic electrons and their influence on the middle atmosphere, *J. Atmos. Terr. Phys., 55*, 1619, 1993.

Callis, L. B., D. N. Baker, J. B. Blake, J. D. Lambeth, R. E. Boughner, M. Natarajan, R. W. Klebesadel, and D. J. Gorney, Precipitating relativistic electrons: Their long-term effect on stratospheric odd nitrogen levels, *J. Geophys. Res., 96*, 2939, 1991.

Chenette, D. L., D. W. Datlowe, R. M. Robinson, T. L. Schumaker, R. R. Vondrak, and J. D. Winningham, Atmospheric energy input and ionization by energetic electrons during the geomagnetic storm of 8-9 November 1991, *Geophys. Res. Lett., 20*, 1323, 1993.

Cummer, S. A., T. F. Bell, U. S. Inan, and L. J. Zanetti, VLF remote sensing of the auroral electrojet, *J. Geophys. Res., 101*, 5381, 1996.

Ferguson, J. A., and F. P. Snyder, The segmented waveguide program for long wavelength propagation calculations, *Tech. Doc. 1071*, Nav. Ocean Sys. Cent., San Diego, Calif., 1987.

Galejs, J., *Terrestrial Propagation of Long Electromagnetic Waves*, Pergamon, New York, 1972.

Glukhov, V. S., V. P. Pasko, and U. S. Inan, Relaxation of transient lower ionospheric disturbances caused by lightning-whistler-induced electron precipitation bursts, *J. Geophys. Res., 97*, 16971, 1992.

Inan, U. S., D. L. Carpenter, R. A. Helliwell, and J. P. Katsufrakis, Subionospheric VLF/LF phase perturbations produced by lightning-whistler induced particle precipitation, *J. Geophys. Res., 90*, 7457, 1985.

Kikuchi, T., and D. S. Evans, Quantitative study of substorm-associated VLF phase anomalies and precipitating energetic electrons on November 13, 1979, *J. Geophys. Res.*, 88, 871, 1983.

Lev-Tov, S. J., U. S. Inan, and T. F. Bell, Altitude profiles of localized *D* region density disturbances produced in lightning-induced electron precipitation events, *J. Geophys. Res., 100*, 21375, 1995.

Potemra, T. A., and T. J. Rosenberg, VLF propagation disturbances and electron precipitation at mid-latitudes, *J. Geophys. Res., 78*, 1572, 1973.

Reagan, J. B., R. E. Meyerott, R. C. Gunton, W. L. Imhof, E. E. Gaines, and T. R. Larsen, Modeling of the ambient and disturbed ionospheric media pertinent to ELF/VLF propagation, paper presented at NATO-AGARD Meeting on Medium, Long, and Very Long Wave Propagation, Brussels, Belgium, Sept. 1981.

Rees, M. H., Auroral ionization and excitation by incident energetic electrons, *Planet. Space Sci., 11*, 1209, 1963.

Rees, M. H., *Physics and Chemistry of the Upper Atmosphere*, Cambridge Univ. Press, New York, 1989.

Ringlee, R. J., Geomagnetic effects on power systems, *IEEE Power Eng. Rev., 9*, 6, 1989.

Swanson, E. R., Omega, *Proc. IEEE, 71*, 1140, 1983.

Thomson, N. R., Experimental daytime VLF ionospheric parameters, *J. Atmos. Terr. Phys., 55*, 173, 1993.

Winningham, J. D., et al., The UARS particle environment monitor, *J. Geophys. Res., 98*, 10,649, 1993.

T. F. Bell, S. A. Cummer, and U. S. Inan, Space, Telecommunications, and Radioscience Laboratory, Stanford University, Durand 324, Stanford, CA 94305-9515.

D. L. Chenette, Lockheed Martin Missiles and Space, Advanced Technology Center, Organization H1-11, Bldg. 252, 3251 Hanover Street, Palo Alto, CA 94304.

(Received September 6, 1996; revised November 27, 1996; accepted November 27, 1996.)